Z. Phys. A 356, 263–279 (1996)

ZEITSCHRIFT
FÜR PHYSIK A
© Springer-Verlag 1996

Interpretation and quality of the tilted axis cranking approximation

Stefan Frauendorf [1], **Jie Meng** [1,2,*]

[1] Institut für Kern- und Hadronenphysik, Forschungszentrum Rossendorf e. V., Postfach 510119, D-01314 Dresden, Germany
[2] Institute of Theoretical Physics, Chinese Academy of Science, Beijing 100080, People's Republic of China

Received: 12 June 1996
Communicated by B. Herskind

Abstract. Comparing with the exact solutions of the model system of one and two particles coupled to an axial rotor, the quality of the semi classical tilted axis cranking approximation is investigated. Extensive comparisons of the energies and $M1$ and $E2$ transition probabilities are carried out for the lowest bands. Very good agreement is found, except near band crossings. Various recipes to take into account finite K within the frame of the usual principal axis cranking are included into the comparison. A set of rules is suggested that permits to construct the excited bands from the cranking configurations, avoiding spurious states.

PACS: 21.60.Ev; 21.60.Jz

1 Introduction

Tilted Axis Cranking (TAC) is a systematic microscopic approach to high spin physics, which provides a semi classical description of the energies and the intra band transition matrix elements for both high-K and low-K bands. After the existence of tilted solutions for a fixed shape had been demonstrated in [1], the interpretation of the solutions has been given in [2, 3], where also the stability of the solutions with respect to deformation has been shown. The method has turned out to be successful in describing the γ-spectra and transition rates of rapidly rotating nuclei (cf. e.g. [4, 5, 6]). As a complement to the standard Principal Axis Cranking (PAC) (e.g. [7]), which describes the $\Delta I = 2$ bands with good signature, the TAC approach permits to calculate the $\Delta I = 1$ bands, staying completely within the microscopic mean field approximation. Such bands are quite common in deformed nuclei. The PAC is a special case of the more general TAC.

Cranking mean field theories are based on the classical treatment of the total angular momentum and the assumption of uniform rotation, which have the consequence that angular momentum conservation is violated. The contact with the quantal spectra is made by means of semi classical expressions for the energy and transition matrix elements. Hence, it seems to be important to investigate how well these approximations work for the description of the experimental observables. There is also the problem of how to construct the excitation spectrum from the TAC quasi particle levels avoiding spurious states. In order to study these questions we start from the Particle Rotor Model (PRM) (c.f. e.g. [8]), which treats the quantal angular momentum dynamics correctly. Introducing to this model the same kind of approximations used for the fully microscopic cranking theory, the TAC version [2] of the model system of a rotor core coupled to a few particles is derived. Comparing the exact PRM solution with the TAC calculations, the quality of the approximation is studied. We study the cases of one and two quasi particles in a j-shell coupled to the axial rotor. These are simple enough to find the exact PRM solution numerically and permit to model the most important angular momentum coupling schemes met in rapidly rotating nuclei. Both energies and intra band transition probabilities are compared. The classification of excited states and ways to avoid spurious states in the spectrum are addressed.

The paper is organized as follows: In Sect. 2 we briefly outline the axial PRM for the model systems we are studying and describe the TAC approximation in the PRM context. The detailed comparisons of axial PRM and TAC calculations for the yrast bands are given in Sect. 3. There, also the construction of the excitation spectrum is discussed and the excited bands of the PRM and TAC are compared. In Sect. 4 previous descriptions of high-K bands using the PAC scheme [9, 10, 12] are compared with the PRM and the TAC.

* *Present address:* Alexander von Humboldt fellow, Physik-Department der Technischen Universität München, D-85747 Garching, Germany

2 Formulation of the models

2.1 Two quasi particles in a single j-shell coupled to an axial symmetric rotor

The PRM Hamiltonian [8] is given by

$$H = h + H_{\text{rotor}}, \quad h = h_p + h_n. \tag{1}$$

For convenience we will call one particle a proton (p) and the other a neutron (n). The formalism is exactly the same for two protons or neutrons in different j-shells. The case of two equivalent particles is also covered by the expressions below, however the Pauli principle must be taken into account in constructing the PRM basis states and the TAC configurations.

Expressing the angular momentum of the rotor by the total angular momentum I_ν and the angular momentum j_ν of the extra particles,

$$R_\nu = I_\nu - j_\nu, \quad j_\nu = j_{\nu p} + j_{\nu n} \tag{2}$$

the axial rotor Hamiltonian reads

$$H_{\text{rotor}} = \sum_{\nu=1,2} \frac{(I_\nu - j_\nu)^2}{2\mathscr{J}}, \tag{3}$$

where $\mathscr{J}$ is the moment of inertia of the rotor and the symmetry axis is chosen to be 3. The j-shell single particle Hamiltonians, denoted by h_p or h_n, are

$$h_{p(n)} = \pm \tfrac{1}{2} C_{p(n)} j^2_{3\,p(n)}, \tag{4}$$

where the upper sign refers to a particle and the lower one to a hole. The parameter $C_{p(n)}$ controls the level splitting in the deformed field. Pairing is treated by means of the BCS-quasiparticle Hamiltonians

$$h_{p(n)} = \sqrt{(\tfrac{1}{2} C_{p(n)} j^2_{3\,p(n)} - \lambda_{p(n)})^2 + \Delta^2_{p(n)}}. \tag{5}$$

The parameters $\lambda_{p(n)}$ and $\Delta_{p(n)}$ are the chemical potential and pairing gap, respectively. The modification of the angular momentum matrix elements by pairing is not taken into account, since it does not lead to any important changes. For the same reason the Coriolis matrix elements are not attenuated. Of course, these simplifications are consistently applied to both the PRM and the TAC, derived below.

The PRM Hamiltonian is diagonalized in the standard basis $|k_p k_n IMK\rangle$, where $|IMK\rangle$ is the Wigner D-function and $|k_p k_n\rangle$ is the product of the j-shell states $|jk\rangle$. The angular momentum projections onto the quantization axis (3-) are denoted by k. The eigenstates are written as states of good signature, i.e.

$$|IM\rangle = \sqrt{\frac{1}{2(1+\delta_{K0})}} \sum_{k_p,k_n} c^I_{k_p,k_n} [|k_p k_n IMK\rangle + (-1)^I |-k_p - k_n IM - K\rangle], \tag{6}$$

where $K = k_p + k_n$ and c_{k_p,k_n} are the expansion coefficients (see [8] for the details). The full recoil term is included into the diagonalization.

The $B(M1)$ values are given by

$$B(M1, I \to I') = \frac{3}{4\pi} |\sum_{\mu,k_p,k_n,k'_p,k'_n} c^{I'}_{k'_p,k'_n} c^I_{k_p,k_n} \times \langle I'K'1\mu \,|\, IK\rangle \langle k'_p k'_n \,|\, (g_p - g_R) j_{p\mu} + (g_n - g_R) j_{n\mu} \,|\, k_p k_n\rangle|^2, \tag{7}$$

where $\boldsymbol{j}$ is written as a spherical tensor of rank 1,

$$j_\mu = \left(j_0 = j_3, j_{\pm 1} = \frac{\mp (j_1 \pm i j_2)}{\sqrt{2}} \right). \tag{8}$$

Since we are only interested in a comparison of TAC with PRM, we set $|g_{p(n)} - g_R| = 1$, choosing the signs such that large $B(M1)$ values are obtained. The $B(E2)$ values are calculated by means of the expression

$$B(E2) = \frac{5}{16\pi} \left| \sum_{k_p,k_n} c^{I'}_{k_p,k_n} c^I_{k_p,k_n} \langle I'K20 \,|\, IK\rangle \right|^2, \tag{9}$$

setting the square of the intrinsic electric quadrupole moment equal to one.

The case of one quasi particle coupled to the rotor is straightforwardly derived from the formulae above by dropping one particle.

2.2 The TAC approximation

In order to obtain the TAC approximation to the axial PRM we assume:

1. The operator $\boldsymbol{I}$ of the total angular momentum is replaced by the classical vector $\boldsymbol{J}$
2. $\langle \boldsymbol{j}^2 \rangle = \langle \boldsymbol{j} \rangle^2$
3. $J_3 = \langle j_3 \rangle$, $J_2 = 0$, $J_1 = \sqrt{J^2 - J_3^2}$

Assumption 1) expresses the semi classical character of the TAC approximation and assumption 2) its mean field character. The relations 3) are consequences of the axial symmetry: There is no collective angular momentum in 3-direction. The classical vector $\boldsymbol{J}$ can always be chosen such that its second component is equal to zero. The absolute value of the classical angular momentum is denoted by J.

With these assumptions the PRM energy becomes

$$E = \langle h \rangle + \frac{1}{2\mathscr{J}} [J^2 - i_3^2 - 2 i_1 \sqrt{J^2 - i_3^2} + i_1^2 + i_2^2], \tag{10}$$

where we have introduced the expectation values $i_\nu = \langle j_\nu \rangle$ of the particle angular momenta (alignments). The expectation values are taken with respect to the product wave function

$$|\rangle = |p\rangle|n\rangle = \sum_{k_p} c_{k_p} |k_p\rangle \sum_{k_n} c_{k_n} |k_n\rangle. \tag{11}$$

The variation $\delta E = 0$ for fixed J with respect to the amplitudes c_k (quasi particle wave functions) leads to the

eigenvalue problem

$$\left(h+\frac{1}{\mathscr{J}}[-i_3j_3-(\sqrt{J^2-i_3^2}+i_1)j_1+\frac{i_1i_3}{\sqrt{J^2-i_3^2}}j_3 + i_2j_2]\right)|\rangle = e'|\rangle\,. \tag{12}$$

This equation can be written as

$$h'|\rangle = e'|\rangle, \quad h' = h - \boldsymbol{\omega}\cdot\boldsymbol{j} \tag{13}$$

with the definition of the angular velocity $\boldsymbol{\omega}$

$$\boldsymbol{\omega} = \left(\sqrt{J^2-i_3^2}-i_1, 0, i_3-\frac{i_1i_3}{\sqrt{J^2-i_3^2}}\right)\Big/\mathscr{J}. \tag{14}$$

The choice $\omega_2 = 0$ implies that $i_2 = 0$, in accordance with assumption 3). Thus, the variational problem (12) is equivalent with the TAC eigenvalue problem (13) and the two self consistency eqs. (14) for the angular velocity. These can be rewritten as

$$\frac{\omega_1}{\omega_3} = \frac{J_1(1-i_1/J_1)}{J_3(1-i_1/J_1)} = \frac{J_1}{J_3} \equiv \tan\vartheta \tag{15}$$

and

$$J = \frac{i_1}{\sin\vartheta} + \omega\mathscr{J}. \tag{16}$$

Eq. (15) is the TAC condition [2, 3, 4] that $\boldsymbol{\omega}$ and $\boldsymbol{J}$ must be parallel at the point of self consistency (energy minimum). It fixes the tilt angle ϑ, which is the angle of total angular momentum $\boldsymbol{J}$ with the 3-axis. Equation (16) provides the relation between ω and J.

Thus, it is shown that the assumptions 1) and 2) lead in fact to the TAC version [2] that approximates the PRM. Let us represent it in the same way as full mean field TAC [3,4] is formulated. The quasi particle states are found by diagonalization of the qp. Routhian

$$h' = h - \omega_3 j_3 - \omega_1 j_1 = h - \omega(\sin\vartheta j_1 + \cos\vartheta j_3) \tag{17}$$

The tilt angle is determined by making $\boldsymbol{\omega}$ parallel to $\boldsymbol{J}$. This is equivalent with minimizing the total Routhian

$$E' = \langle h'\rangle - \tfrac{1}{2}\mathscr{J}(\omega\sin\vartheta)^2 \tag{18}$$

with respect to ϑ at fixed ω. The expectation value of the total angular momentum in the intrinsic frame system is given by the expressions

$$J_1 = i_1 + \sin\vartheta\omega\mathscr{J}, \quad J_3 = i_3, \quad J = \sqrt{J_1^2+J_3^2}. \tag{19}$$

The total energy E (lab. frame) and the total Routhian E' (rotating frame) are related by the standard canonical eqs.

$$E = E' + \omega J, \quad \frac{dE}{dJ} = \omega, \quad \frac{dE'}{d\omega} = -J. \tag{20}$$

Naturally, the TAC expressions derived from PRM contain a core contribution in addition to the quasi particle part, whereas in the full TAC all energy and angular momentum comes from the quasi particles. The PRM version of TAC is discussed in detail in [2].

2.3 Relation of TAC to the rotational states

Before comparing the smooth functions $J(\omega)$, $E(J)$, … obtained in TAC with the discrete values I, $E(I)$, … calculated in the PRM, the relationship between the classical TAC quantities and the quantal PRM quantities must be established. One must distinguish between two cases:

1. TAC solution $|\omega\rangle$: The energy minimum lies at a tilt angle ϑ that is different from 0° or 90°. The signature symmetry is broken and the quasi particle configuration is wave packet composed of all possible I-states. It is associated with a $\Delta I = 1$ rotational band of parity π, whose states are inter-connected by strong $M1$ and $E2$ transitions.
2. PAC solution $|\alpha,\omega\rangle$: The energy minimum lies at the tilt angle $\vartheta = 90^\circ$. The signature α is a good quantum number and the quasi particle configuration is wave packet composed of all possible $I = \alpha$ mod 2 states. It is associated with a $\Delta I = 2$ rotational band of parity π and spin $I = \alpha$ mod 2, whose states are inter-connected by strong E2-transitions.

This distinction is a consequence of the mean field approximation. The two types of solutions with different symmetry have to be interpreted differently, leading to well known problems for the transitional cases. The gradual appearance of signature splitting along a band cannot be described by the TAC. This question will be discussed in more detail below.

In order to include the lowest order quantal correction the spin I of the PRM must be associated with the angular momentum $J(\omega) - 1/2$ of TAC [8, 10]. For example, $E(I)$ of the PRM is compared with $E(J = I + 1/2)$ calculated in TAC. The inclusion of this quantal correction considerably improves the agreement between PRM and TAC.

Analyzing the experiments it is often useful to transform the quantal values of energy and spin to the frequency ω and the Routhians E' of the cranking theory [10]. We will do the same with our PRM results. In the case of a $\Delta I = 1$ band we use

$$J = I, \quad \omega = E(I) - E(I-1),$$
$$E' = \tfrac{1}{2}[E(I) + E(I-1)] - \omega J. \tag{21}$$

Due to the quantal correction one must associate J with $I + \frac{1}{2}$, while the rotational frequency ω is the transition energy from I to $I - 1$ corresponding to the mean value $I - \frac{1}{2}$. Hence, the angular momentum J of the transition is given by I, the upper spin value.

For $\Delta I = 2$ bands with signature splitting we use

$$J = I - \tfrac{1}{2}, \quad \omega = \tfrac{1}{2}[E(I) - E(I-2)],$$
$$E' = \tfrac{1}{2}[E(I) + E(I-2)] - \omega J. \tag{22}$$

This corresponds to the prescription of [10], *setting* $K = 0$ (no projection of the angular momentum on the 1-axis). Equations (21) and (22) provide discrete points $J(\omega)$ and $E'(\omega)$ that are compared with the corresponding points on the continuous curves calculated by means of TAC. In some figs. we shall show continuous functions $E'(\omega)$ for the PRM that are obtained by interpolation from the discrete points.

By semi classical correspondence one finds [2, 3, 12] for the intra band M1-transition strength[1]

$$B(M1) = \frac{3}{8\pi}[\sin\vartheta((g_p - g_R)i_{3p} + (g_n - g_R)i_{3n}) - \cos\vartheta((g_p - g_R)i_{1p} + (g_n - g_R)i_{1n})]^2 \quad (23)$$

The $B(M1)$ value calculated at angular momentum $J(\omega) = I$ must be compared with $B(M1, I \to I - 1)$ of the PRM (cf. discussion of the definition of ω). The stretched $BE(E2)$ values are given by [2, 4, 12]:[2]

$$B(E2) = \frac{15}{128\pi}(\sin\vartheta)^4 \quad (24)$$

The TAC value calculated for $J(\omega) = I - 1/2$ is compared to the $B(E2, I \to I - 2)$ value in the PRM.

The expression (24) for the $B(E2)$ values is applicable both for TAC and PAC solutions. The expression (23) for the $B(M1)$ values gives 0 for PAC solutions, because the transversal component of the magnetic vector is zero for symmetry reasons. In this case the two branches of the band among which the magnetic transition takes place must be interpreted as two intrinsic configurations with opposite signature. The $B(M1)$ value is then given by the expression suggested by Hamamoto and Sagawa [14][3]

$$B(M1) = \frac{3}{4\pi}\langle 1|(g_\tau - g_R)\, j_{\pm 1,\tau}|2\rangle^2, \quad (25)$$

where τ is p or n depending on whether the proton or the neutron changes its configuration and $j_{\pm 1}$ are the spherical components defined by (8), *but with respect to the* 1*-axis.*

3 Comparison of the PRM and TAC

Particles, holes and quasi particles in the $h_{11/2}$ shell are studied as examples. Different coupling schemes are considered, which correspond to different choices of the constant C in the single particle Hamiltonian (4). We consider two values, $|C| = 0.25$ MeV and 0.10 MeV corresponding to a well deformed and weakly deformed nucleus ($\beta \approx 0.25$ and 0.1), respectively. Let us adopt the classification of coupling schemes suggested in [15]. For prolate shape, the value $C = 0.25$ MeV corresponds to a particle at the bottom of the shell, which becomes very easily rotational aligned (RAL-rotational aligned). The value $C = -0.25$ MeV corresponds to a hole at the top of the shell, which is aligned with the symmetry axis of the deformed field (DAL-deformation aligned). For oblate shape the particle and the hole change their roles. A mid-shell quasi particle ($k \approx 7/2$) is modeled by the quasi particle Hamiltonian (5) with $C = 0.25$ MeV, $\Delta = 0.8$ MeV and $\lambda = 2$ MeV. It corresponds to a coupling that prefers an angle of about 45° with respect to the 3-axis (FAL-Fermi aligned). In principle the same classification applies for the small deformation. However, the rotation perturbs the idealized schemes considerably.

To be realistic, the core moment of inertia is chosen to be $\mathcal{J} = 30$ and $15\,\text{MeV}^{-1}$ for the large and the small deformation, respectively. The agreement between TAC and PRM, discussed below, is not sensitive to the value of $\mathcal{J}$. In order to make small energy differences better visible, the term $-\theta\omega^2/2$, with $\theta = 30\,\text{MeV}^{-1}$ (rigid rotor Routhian) is subtracted from both the TAC and the PRM Routhians shown in Figs. 14, 15 and 16. It represents just a shift of all energies by the same amount and θ must not be confused with the moment of inertia $\mathcal{J}$ of the PRM.

3.1 One particle or hole

The upper panel of Fig. 1 shows the single particle Routhians. The slope of the trajectories is proportional to the component of the angular momentum perpendicular to the vector $\boldsymbol{\omega}$,

$$\frac{\partial e'(\omega, \vartheta)}{\partial\vartheta} = \omega(-\cos\vartheta i_1 + \sin\vartheta i_3) = -\omega i_\perp. \quad (26)$$

A particle in the lowest states prefers $\vartheta = 90°$, i.e. RAL coupling. A hole in the highest states prefers $\vartheta = 0°$, i.e. DAL coupling. The lowest state in lower panel is a mid-shell quasi particle that obeys FAL coupling. It has its

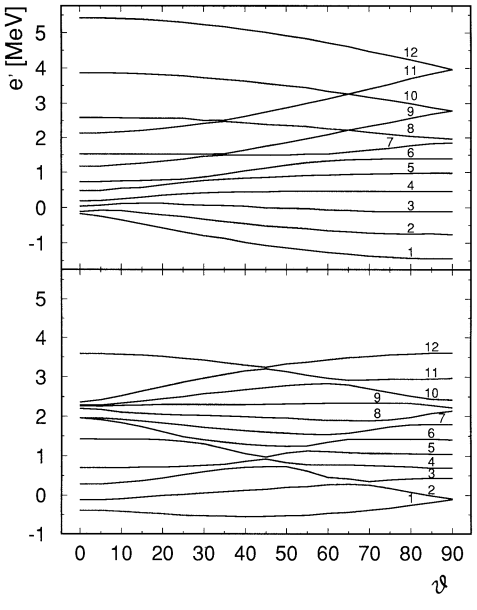

Fig. 1. Upper panel: Single particle Routhians as functions of the tilt angle ϑ for $C = 0.25$ MeV and $\omega = 0.3$ MeV. Lower panel: Quasi particle Routhians for the same parameters and $\Delta = 0.8$ MeV and $\lambda = 2$ MeV. For $\vartheta = 90°$ the signature α is $-1/2$ for the levels with odd numbers and 1/2 for the others

[1] Deriving (23) from the microscopic expression (14) of [3], one singles out the contributions of the valence particles and defines the rest as the core contribution. Introducing $\boldsymbol{\mu}_p = g_p \boldsymbol{i}_p$, $\boldsymbol{\mu}_n = g_n \boldsymbol{i}_n$, $\boldsymbol{\mu}_R = g_R \boldsymbol{R}$ and using that $\boldsymbol{R} = \boldsymbol{J} - \boldsymbol{i}_p - \boldsymbol{i}_n$ implies $R_\perp = -(i_p + i_n)_\perp$, (23) is obtained

[2] [4] contains an unfortunate misprint, missing a factor of 1/4

[3] The expression $\boldsymbol{\mu}_{n\pm 1} = (g_\tau - g_R) j_{\pm 1,\tau}$ used for the magnetic moment operator accounts for the conservation of angular momentum. It can easily be guessed from the quantal expressions given in [8]

minimum around $\vartheta = 45^\circ$. Since the curve is rather flat, $i_\perp$ is relatively small, i.e. the FAL quasi particles tend to align with $\boldsymbol{\omega}$.

In addition to the particle energies, the total Routhian $E'(\vartheta)$ in (18) contains the core term $-\frac{1}{2}\mathcal{J}(\omega \sin\vartheta)^2$, which is minimal at $\vartheta = 90^\circ$. It shifts the minimum of $E'(\vartheta)$ towards the 1-axis, which is the direction of the collective angular momentum $\boldsymbol{R}$. Figure 2 shows $E'(\vartheta)$ for the case of one hole.

Not all minima of $E'(\vartheta)$ correspond to a band. If $\vartheta = 0^\circ$, the wave function does not depend on ω. It represents one and the same state, the band head. Take the case of a hole shown in Fig. 2 as an example. As long as the curvature of the hole state (negative curvature of the highest level in Fig. 1) is larger than $\mathcal{J}\omega^2$ (curvature of the collective term) the minimum remains at $\vartheta = 0^\circ$ and the band has not yet started. When the two curvatures are equal the band head is reached. At this point the minimum bifurcates from a maximum at $\vartheta = 0^\circ$, moving towards 90°. The movement of the minimum can be seen in the Fig. 2. For small frequencies the curves $E'(\vartheta)$ become very shallow. Superficially, one could conclude that there will be large fluctuations in the orientation and the TAC solution becomes invalid. However, this is not the case, because at the band head the PRM wave function reduces to one component with $k = 11/2$, i.e. it becomes narrow instead of wide. This means that not only the curvature of the function $E'(\vartheta)$ goes to zero but also the mass coefficient associated with the oscillation in ϑ, such that the width of the wave function goes to zero. Thus, the TAC approximation should work well at the band head.

Figure 3 compares the TAC calculations for one particle and one hole with the corresponding PRM ones. In the case of the particle (RAL) only the PAC solution $\vartheta = 90^\circ$ is found. The signature is good, it is, respectively, $\alpha = -1/2$ and $1/2$ for the levels 1 and 2 in Fig. 1. The energies of the two PAC configurations agree well with the ones of the two $\Delta I = 2$ bands calculated in the PRM. As suggested in [14], for a PAC solution one has to calculate the $B(M1)$ values as the non-diagonal matrix

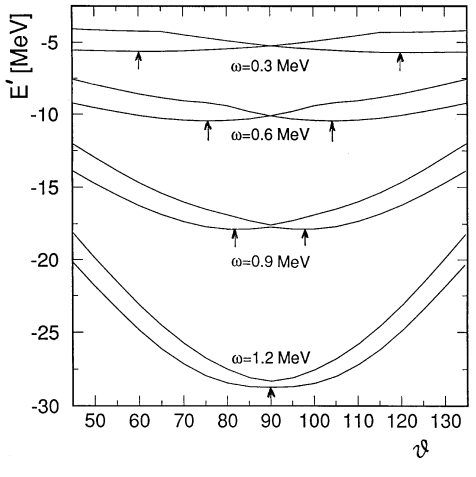

Fig. 2. Total Routhians of the lowest two hole states ($C = -0.25$ MeV) as functions of the tilt angle ϑ for $\omega = 0.3, 0.6, 0.9$ and 1.2 MeV. For $\vartheta = 90^\circ$ the signature is $\alpha = -1/2$ for the lower curve and $1/2$ for the higher one of each pair. The arrows indicate the minima

elements of the $M1$ operator between the states of opposite signature by means of (25). The comparison in Fig. 3 shows fair agreement.

In the case of the hole (DAL), the minima of $E'(\vartheta)$ in Fig. 2 represent the $\Delta I = 1$ TAC band as long as $\vartheta < 90^\circ$. As seen in Fig. 3, the TAC calculation very accurately reproduces both the energies and the $B(M1)$ values, which must now be calculated by means of (23). It is noted that the TAC curve in Fig. 3 starts at $\omega = 0.183$ MeV, where we find the band head (zero curvature at $\vartheta = 0^\circ$ in Fig. 2). In accordance with the discussion above, TAC describes very well both the energies and the transition probabilities near the band head.

At $\omega \approx 0.7$ MeV one notices the onset of signature splitting in the function $J(\omega)$ derived from the PRM. It is more evident in the $B(M1)$ values for the corresponding angular momentum of about 25. Both signatures are attributed to one and the same TAC solution, which provides the mean value with good accuracy. The onset of the staggering is the precursor of the transition $\vartheta \to 90^\circ$, which occurs for $\omega \approx 1.2$ MeV, as seen in Fig. 2. In the cranking approach this transition leads to a discontinuity, because one must switch from the interpretation of the TAC solution as a $\Delta I = 1$ band to the PAC interpretation, where to each configuration of given signature a $\Delta I = 2$ band of the appropriate I is associated.

To formulate a rule that prevents over-counting of states, it is helpful to consider a symmetric graph like Fig. 2. For $\omega < 1.2$ MeV there are always two degenerate minima symmetric to 90°. This is the manifestation of the breaking of the signature symmetry. These two minima generate the $\Delta I = 1$ TAC band, since they may be combined into an odd and an even superposition, corresponding to the two degenerate signature partners $I = 1/2 + 2n$ and $I = -1/2 + 2n$. The left minimum arises from the hole in level 12 (cf. Fig. 1) and the right one from the hole in level 11 continued diabatically through the the crossing at 90°. Hence, the configuration based on a hole in 11 also belongs the $\Delta I = 1$ TAC band. At $\vartheta = 90^\circ$, the upper curve of each pair in Fig. 2 corresponds to a mixture of 50% of level 11 and 50% of level 12. It has an overlap of almost 100% with the signature 1/2 combination of the minima of the lower curves. Consequently, the narrow minimum at 90° in the upper curve of each pair must be considered as spurious. It must be discarded, because it does not represent an additional band.[4]

For $\omega > 1.2$ MeV the two minima in the lower curve of each pair have merged into one at 90°, where the signature is a good quantum number. Now the minima at $\vartheta = 90^\circ$ of *both* the lower and upper configurations of each pair are associated with a $\Delta I = 2$ PAC band. They are interpreted as the two signature partners with $I = \pm 1/2 + 2n$, in the same way as we did for the RAL particle on the levels 1 and 2. The signature splitting is given by the distance between the two curves in Fig. 2 at $\vartheta = 90^\circ$.

Thus, within the TAC theory signature splitting appears suddenly at the change from the TAC to PAC

[4] The kinks in the first excited configuration in Fig. 2 correspond to the crossing of the levels 11 and 10. The branch where the hole is on level 10 does represent an excited band

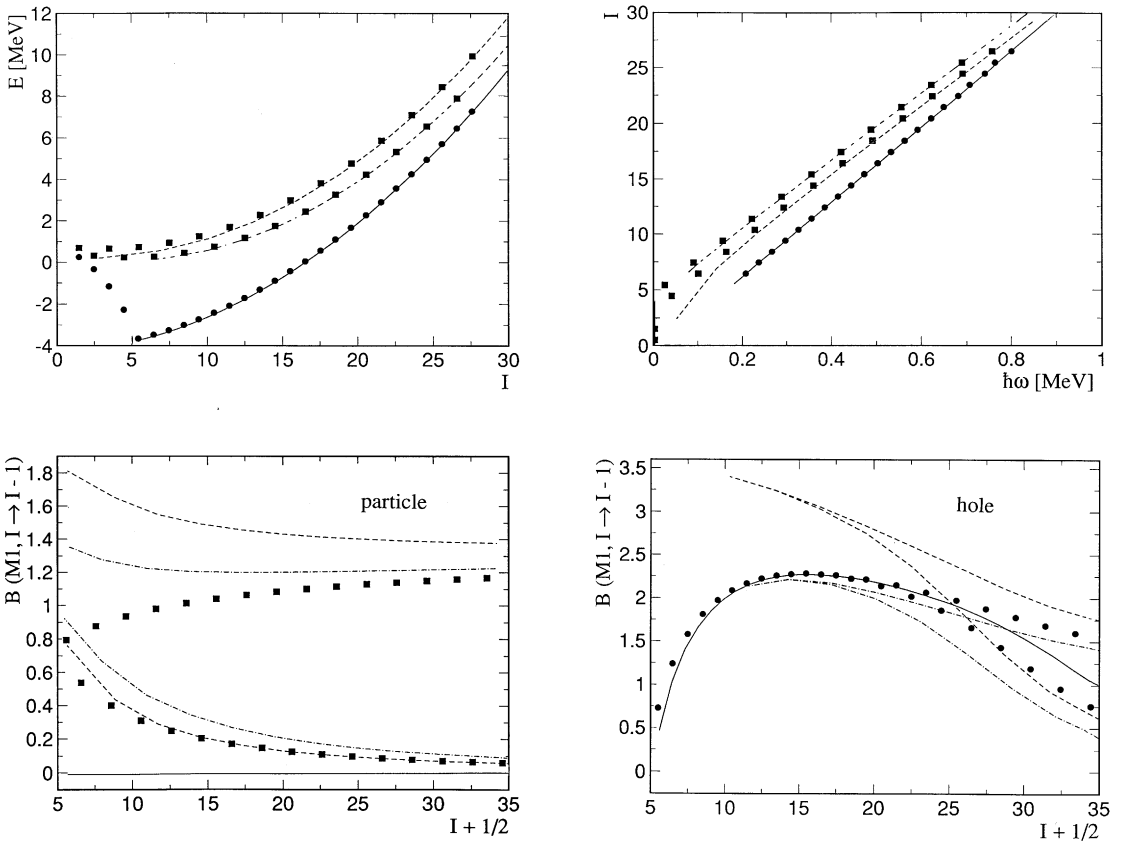

Fig. 3. Energy, angular momentum and $B(M1)$ values of the lowest bands for a particle and a hole coupled to the rotor. Circles: PRM-hole, squares: PRM-particle, full line: TAC-hole, dashed line: PAC-particle. The dashed dotted curve is calculated by means of (37), combining the tilted geometry with the PAC calculation

interpretation. TAC only describes the two limiting cases of no or substantial splitting, the gradual onset cannot be accounted for. Around $\omega = 0.9$ MeV or angular momentum 30 one must switch from the TAC interpretation without signature effects to the PAC interpretation with finite signature effects. The pair of curves for $\omega = 0.9$ MeV can be interpreted in two ways: Either the two minima at 82° and 98° generate the lowest $\Delta I = 1$ band. Then the narrow minimum at $\vartheta = 90^\circ$ of the higher of the two curves must be discarded. Or the minimum and the maximum at $\vartheta = 90^\circ$ are interpreted as the two signature branches. As seen in Fig. 3 the best match of the $B(M1)$ values is achieved if one changes from the TAC to the PAC interpretation near $\omega = 0.9$ MeV, somewhat before the two minima in the lower curve have merged. This can be attributed to the zero point fluctuations.

The signature splitting of the energies is barely visible in Fig. 3. For the FAL quasiparticle, discussed next, one also encounters a noticeable discontinuity in the energies.

3.2 One mid-shell quasi particle

Figure 4 illustrates the case of a quasi particle in the middle of the shell, where pairing must be taken into account. The chemical potential lies between the 7/2 and 9/2 level. The configuration corresponds to a FAL quasi particle on the lowest level in lower panel of Fig. 1. We define the band head from the criterion that in a band the energy must increase with I. For the PRM yrast energies this is the case from the $11/2 \to 9/2$ transition on. The corresponding frequency $\omega = 0.05$ MeV agrees well with the lowest value of ω for which we find a TAC solution. At the band head there is a rapid change from DAL coupling to the FAL coupling. Though the agreement is not perfect, the TAC is still a good approximation near the band head. At $\omega = 0.7$ MeV and $I = 25$ the tilt angle ϑ reaches 90°. The change from the TAC interpretation to the PAC scheme with signature splitting leads to a more pronounced discontinuity in the energies than for the case of one hole discussed above. Up to about spin 18 the TAC solution describes the signature average of the energy and of the $B(M1)$ values well. Above spin 25 the PAC solution becomes a good approximation. Again, the best possible match is achieved around spin 20, somewhat below where the two TAC minima merge into the PAC minimum.

3.3 Yrast band of two holes

The coupling of a DAL proton hole and a DAL neutron hole (both in level 12 of Fig. 1) to the rotor is illustrated in Fig. 5. As seen in Fig. 6, the TAC reproduces the PRM energies and transition probabilities very well. The growth

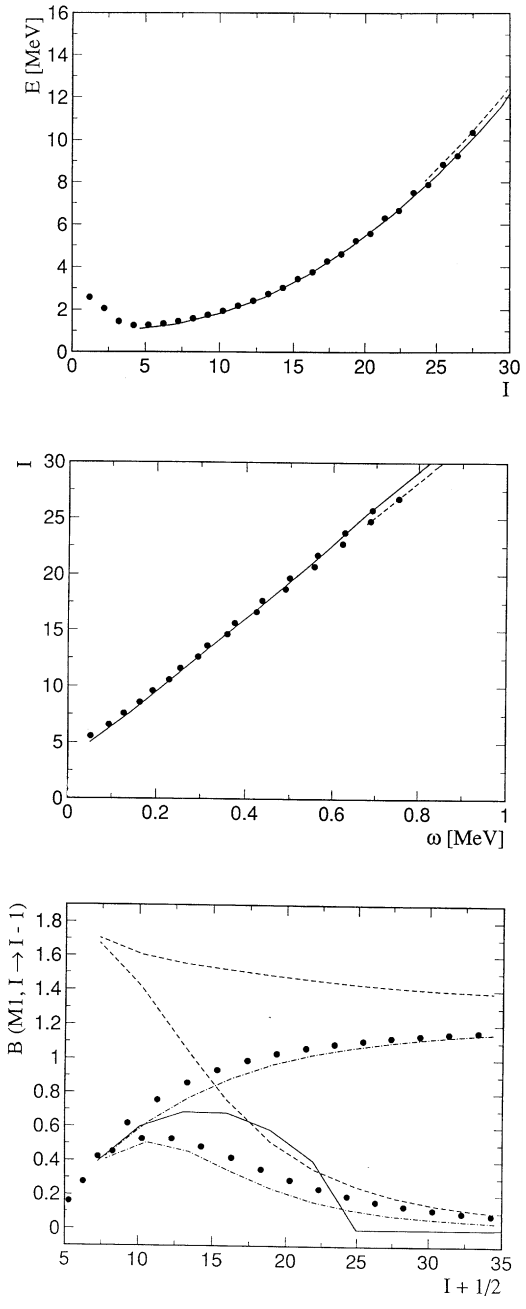

Fig. 4. Energy, angular momentum and $B(M1)$ values of the lowest band for a mid-shell quasi particle. Circles: PRM, full lines: TAC and dashed lines: PAC (in the upper two panels only signature 1/2, $-1/2$ is shown as a full line). The dashed dotted curve is calculated by means of (37), combining the tilted geometry with the PAC calculation

of the $B(M1)$ and $B(E2)$ values reflects the well known strong coupling behavior [8]. The strong coupling limit is obtained from the general expressions (23) and (24) by assuming that $J_3 = K$, $i_{1,\tau} = 0$ and $i_{3,\tau} = k_\tau$, where K and k are kept fixed. Quoting also the exact strong coupling expressions [8], one has

$$B(M1, I \to I') = \frac{3}{4\pi} |\langle I' K' 1\mu | IK\rangle \mu_3|^2 \approx \frac{3}{8\pi} [\sin \vartheta \mu_3]^2, \tag{27}$$

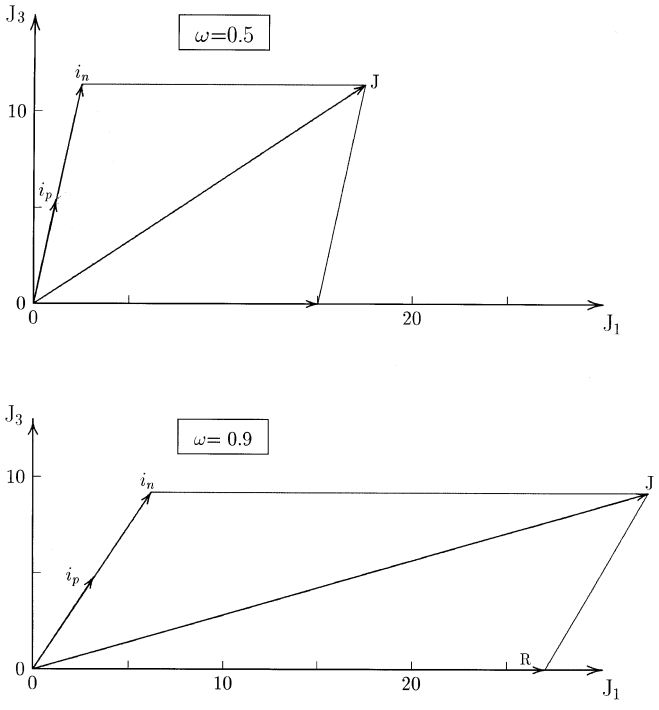

Fig. 5. Geometry of angular momentum for the combination of a proton DAL hole with a neutron DAL hole

$$B(E2, I \to I') = \frac{5}{16\pi} |\langle I' K 20 | IK\rangle|^2 \approx \frac{15}{128\pi} (\sin \vartheta)^4, \tag{28}$$

$$\cos \vartheta = \frac{2K}{I + I' + 1}, \quad \mu_3 = (g_p - g_R) i_{3p} + (g_n - g_R) i_{3n}. \tag{29}$$

The TAC approximates the Clebsch-Gordan coefficients by their asymptotic values.

At larger frequency deviations from the strong coupling limit appear. In Fig. 5, the strong coupling limit corresponds to $\boldsymbol{i}_p$ and $\boldsymbol{i}_n$ being parallel to the 3-axis. It is seen that for increasing ω there is a substantial deviation from this limit developing. This tilt of the vectors $\boldsymbol{i}$ towards $\boldsymbol{J}$ explains the decrease of the $B(M1)$ values at large spin, which are proportional to the square to the transversal component of $\boldsymbol{i}$.

3.4 Yrast band of a particle and a hole

The coupling of a RAL proton (in level 1 of Fig. 1) and a DAL neutron hole (in level 12 of Fig. 1) to the well deformed rotor ($C = 0.25$ MeV) is illustrated by the vector diagram 7. As seen in Fig. 8, TAC approximates the PRM well for the "rotational part" of the yrast sequence, where the energy increases with the angular momentum. Near the minimum of $E(I)$, which represents the band head, the TAC ceases to work. The $B(M1)$ values drop to zero, whereas they continue to grow in the PRM. The problem arises, because the RAL proton dealigns when ω goes to zero. In the PRM it remains rotational aligned even in the region below the minimum. This is a consequence of zero

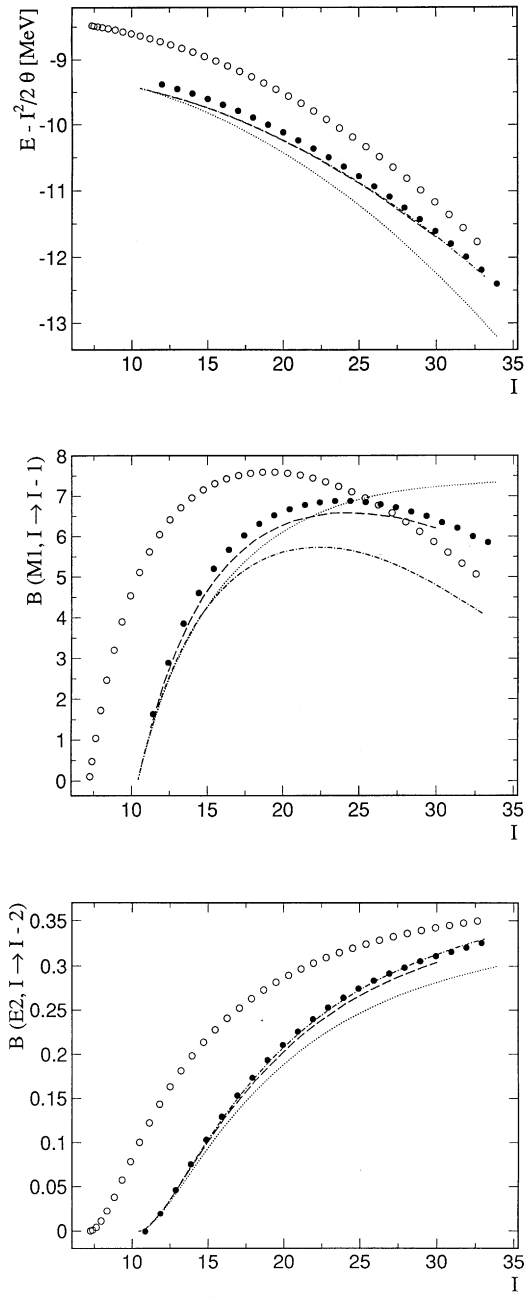

Fig. 6. Energy, $B(M1)$ and $B(E2)$ values of the lowest band for the combination of a proton DAL hole with a neutron DAL hole. Full circles: PRM, dashed line: TAC. A rigid rotor contribution with $\theta = 30\,\mathrm{MeV}^{-1}$ has been subtracted from the energy. Several prescription to treat finite K within the PAC are included. Dotted line: BFFP, open circles: RMB and dashed-dotted: FM

point fluctuations that are not included in TAC. This discrepancy is in contrast to a situation when strong coupling is approached at the band head, like the case of a proton hole combined with a neutron hole, discussed above. In this case TAC works very well near the band head, because ω is finite there.

Figure 9 compares the wave functions of the PRM with the ones of TAC. The upper panel shows the probability of the different projections k of the $h_{11/2}$ single

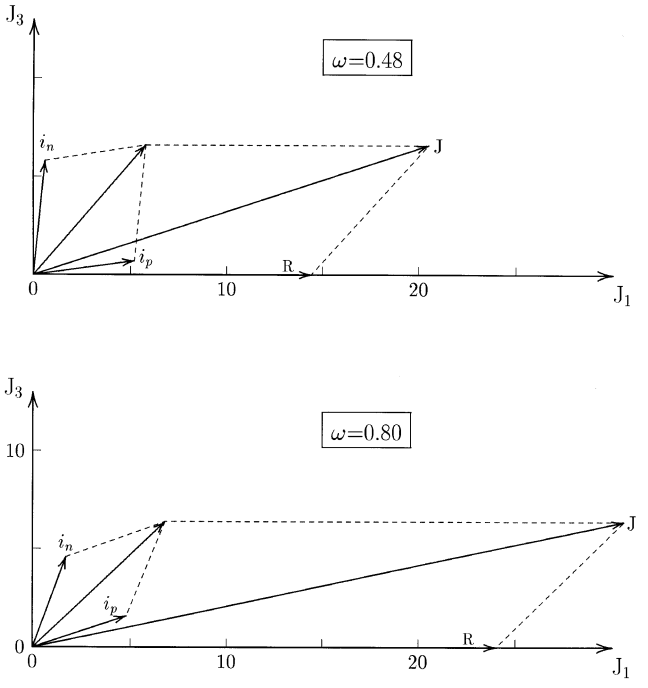

Fig. 7. The geometry of angular momentum for the combination of a proton RAL hole with a neutron DAL hole

particle states[5] and the lower one shows the distribution of the total projection $K = k_p + k_n$. The mean value of K of the PRM distribution is close to the J_3 value of TAC. The distribution of the PRM are wider than the ones of the TAC, i.e. the PRM has a stronger K-mixing than TAC. This is a consequence of the zero point fluctuations missing in TAC. The fact that the distributions have similar centroids explains the good results of TAC for the energies, $B(M1)$ and $B(E2)$ values, because they are diagonal matrix elements that are mainly determined by the mean values of the angular momentum contributions. For non-diagonal transition matrix elements the difference in the widths of the distributions are expected to ensue stronger deviations.

Figure 8 also displays the weakly deformed case $C = 0.1$ MeV. As illustrated by the vector diagram 10, only at the band head the classification into a RAL proton and a DAL neutron hole makes sense. At higher spin there is a strong reorientation of both $\boldsymbol{i}_p$ and $\boldsymbol{i}_n$ towards the $\boldsymbol{J}$ axis. This is the characteristic shears mechanism [3, 6] discovered recently in the light Pb-isotopes. Also in this case, the agreement between PRM and TAC is quite reasonable. There is a transition TAC $\rightarrow$ PAC around $I = 15$. It is seen as the onset of signature splitting in the PRM results. The tilt angle becomes $\vartheta = 90^\circ$ near $\omega = 0.5$ MeV. The same problems as discussed for the one particle

[5] The PRM wave function is "desymmetrized". This means we solve the PRM problem within the basis (6) and additionally within the basis of "wrong signature" that combines the two terms $\pm K$ with the opposite sign. The two solutions are degenerated (if the signature splitting is negligible). The superposition of the two solutions with equal weights gives the asymmetric k-distribution that can directly be compared to the TAC

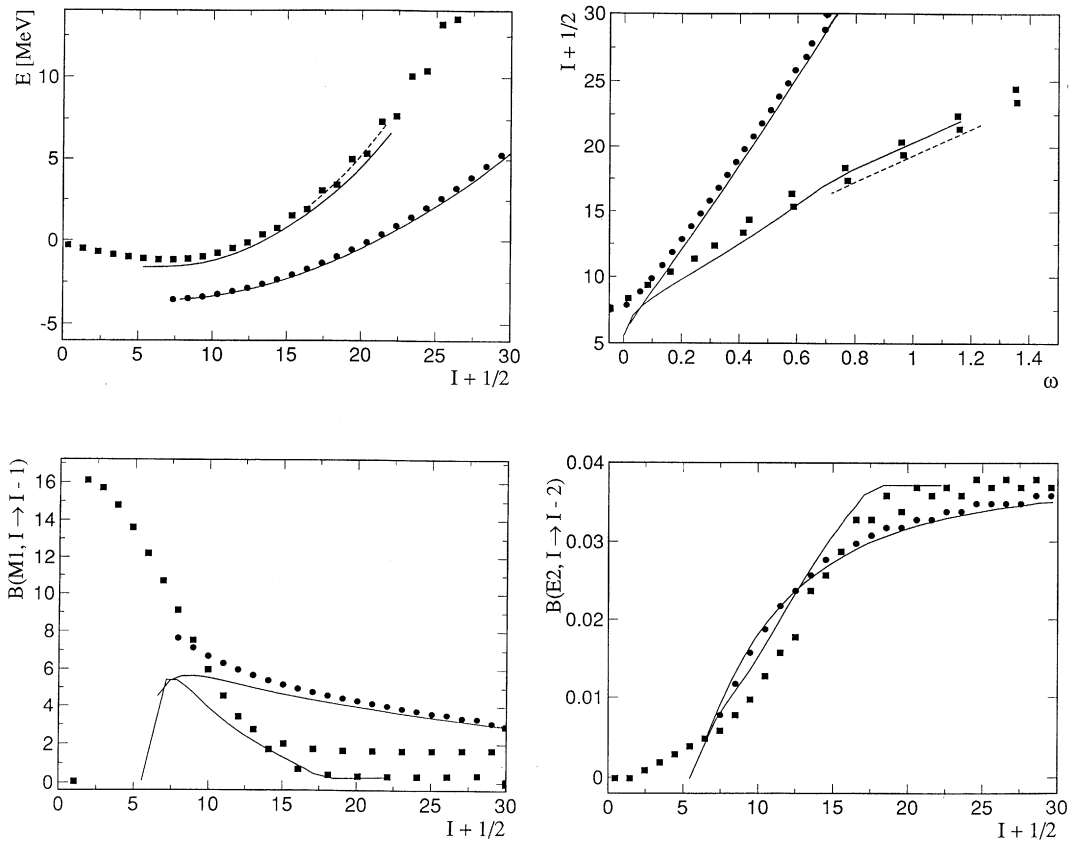

Fig. 8. Energy, angular momentum, $B(M1)$ and $B(E2)$ values for lowest band of the combination of a proton RAL hole with a neutron DAL hole. Circles: PRM $C = 0.25$ MeV, squares: PRM $C = 0.10$ MeV, full lines: TAC, dashed lines: PAC signature

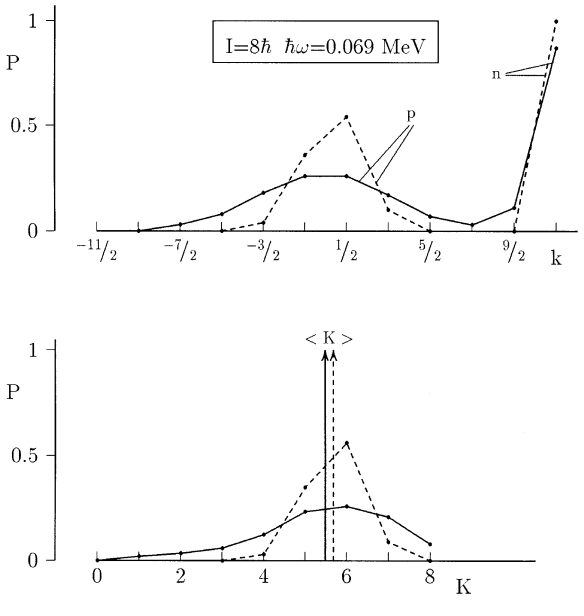

Fig. 9. The structure of the wave function for TAC (dashed) and PRM (full). Upper panel: The k-distributions for the proton and neutron. Lower panel: The distribution total $K = k1 + k2$. The average K values are indicated by the arrows. For obtaining the PRM values the wavefunction has been desymmetrized (cf. footnote p. 12)

case arise. The signature splitting appears as a sudden jump.

The physics of shears bands has been discussed on the basis of the TAC [3, 6]. The comparison shows that within PRM, which treats the angular momentum as a quantal quantity, the shears mechanism shows up in the same way as in the semi classical TAC. This is demonstrated by the vector diagram 10, where we compare the angular momentum expectation values calculated in TAC with the ones calculated from the PRM wave functions. The higher frequency is chosen just below the value where the TAC solution collapses into the PAC (i.e. $\vartheta \to 90°$). In our model study we consider only one particle and one hole, each carrying 5.5 units of angular momentum. Many of the shears bands in the Pb-isotopes are composed of at least two particles and two holes, each of which carrying a similar amount of angular momentum. For these bands the TAC solution survives to higher frequencies. Some of the observed configurations are possibly one particle–one hole excitations. Like the one we study here, they seem to develop signature splitting [6].

3.5 Yrast band of a mid-shell proton and neutron

Figures 11 and 12 shows the combination of a mid-shell FAL quasi proton and a mid-shell FAL quasi neutron

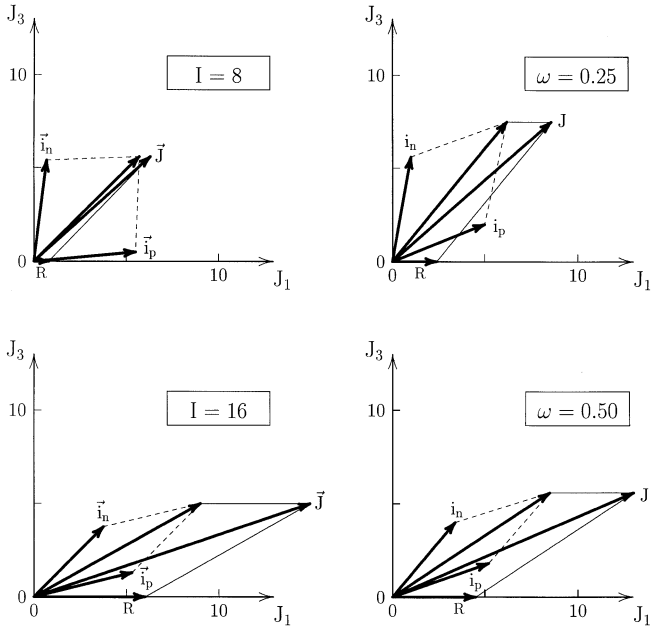

Fig. 10. The geometry of angular momentum for shears bands. The left panel ($\hbar\omega = 0.25, 0.50$ MeV) shows the TAC calculation and the right panel ($I = 8, 14$) the PRM calculation. For obtaining the PRM values the PRM wavefunction has been desymmetrized (cf. footnote p. 12)

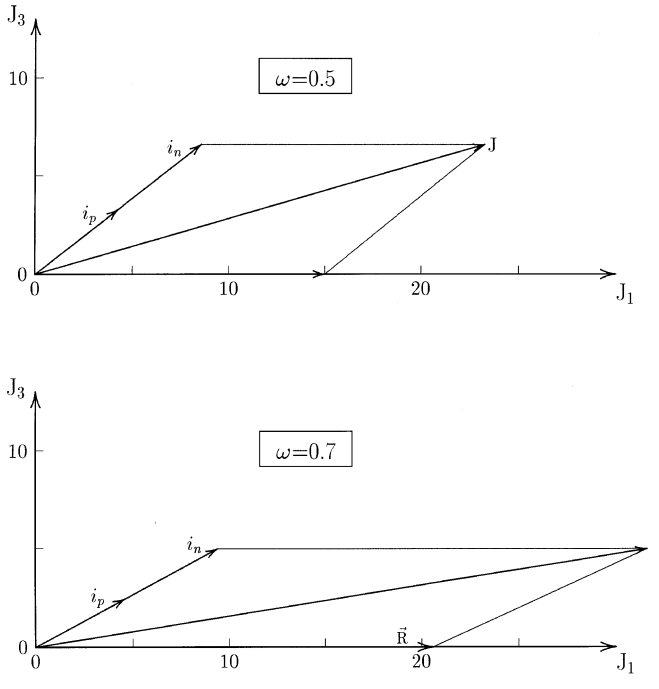

Fig. 11. The geometry of angular momentum for the combination of a FAL quasi proton with a FAL quasi neutron

(both in level 1 of Fig. 1 lower panel). As illustrated by the vector diagram 11, the two quasi particles have an orientation angle of about 45°, which somewhat increases with the frequency. This is characteristic for the FAL coupling. Also for this coupling, the agreement between PRM and TAC is quite good. When calculating the $B(M1)$ values for the PAC limit one must take into account the fact that the first excited configuration is twofold degenerated (proton or neutron excited). These two configurations are mixed by the PRM Hamiltonian. Accordingly, one must calculate the non-diagonal matrix element (25) between the PAC states $|1\rangle$ and $(|2\rangle + |2'\rangle)/\sqrt{2}$.

3.6 Excited bands

Figure 13 shows $E'(\omega = 0.5\,\text{MeV}, \vartheta)$ for the lowest configurations of two DAL holes. In order to avoid over counting states, we must extend the discussion started in Sect. 3.1. Consider first the bundle of configurations 1–4, generated by putting the neutron and a proton holes on the levels 11 and 12 in Fig. 1. The configurations 2 and 3 are degenerated. There are four configurations of given signature at $\vartheta = 90°$, two with even I and two with odd I. This is the number of $\Delta I = 2$ bands that is associated with this bundle. In the TAC regime, the two symmetric minima of configurations 1 and 4 generate a $K = 11$, $\Delta I = 1$ band. The two minima of the configurations 2 and 3 at 90° generate a $K = 0$, $\Delta I = 1$ band. This exhausts the number of physical configurations. The kink formed by 1 and 4 at 90° must be discarded. With increasing ω, the minima of 1 and 4 move towards 90°. We keep the TAC interpretation until these two minima approach 90°. Then we shift to the PAC interpretation, where all configurations at 90° are accepted. Now the good signature α confines I. Configuration 1 has $\alpha = 1 = (-1/2) + (-1/2)$ (odd spin) followed by the degenerate configurations 2 and 3 with $\alpha = 0 = (-1/2) + (1/2)$, $(1/2) + (-1/2)$ (even spin) and configuration 4 with $\alpha = 1 = (1/2) + (1/2)$ (odd spin). It is important that the shift from the TAC to PAC interpretation is made for *the whole bundle at the same* ω. The degenerate configurations 5 and 6 are generated by putting the proton and neutron holes on levels 12 and 10 and the configurations 7 and 8 by putting them on 9 and 11. They form two $K = 10$, $\Delta I = 1$ bands.

Figure 14 shows that this interpretation leads to the right spectrum and that TAC provides a very good description of the PRM energies and transition probabilities. The only discrepancy is the energy difference between the two $K = 10$ bands. It is caused by the two body part of the recoil term in the PRM Hamiltonian, which is not taken into account in TAC. The $B(M1)$ and $B(E2)$ values for the excited bands are well reproduced by TAC. The transition to the PAC regime is not reached in this example, but it will be seen in the following ones.

The excitation spectrum of a RAL proton combined with a DAL neutron hole is illustrated in Fig. 15. The left column of Table 1 lists the configurations. The configurations 1 and 2 correspond to the proton on level 1 in Fig. 1 and the neutron hole on 11 or 12. Configurations 3, 4 and 5, 6 correspond to the neutron hole and 11 and 12 combined with the proton on levels 2 and 3, respectively. According to the rules, these configurations generate the three lowest $\Delta I = 1$ bands. It is noted that for $\omega = 0.1$ MeV band (1, 2) has already started (minimum at 54°)

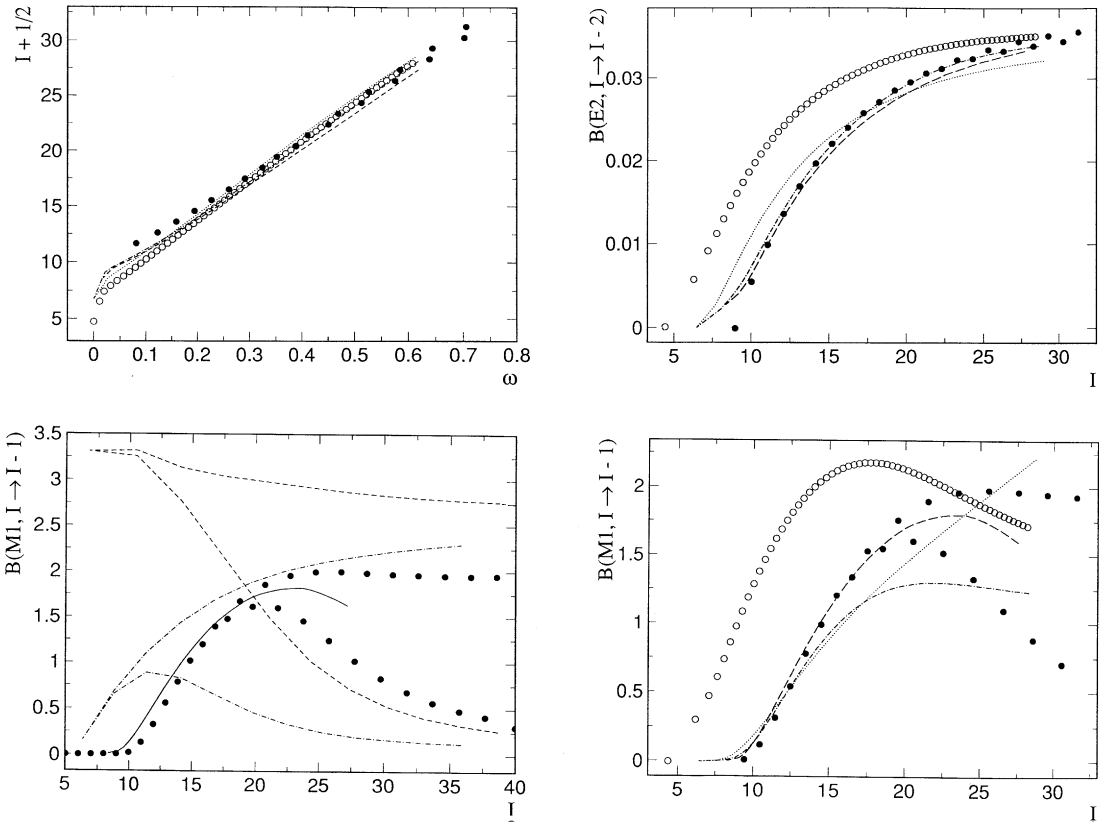

Fig. 12. Angular momentum, $B(E2)$, and $B(M1)$ values for the lowest band of the combination of a FAL quasi proton with a FAL quasi neutron. Full circles: PRM. Left lower panel: Full line: TAC, dashed lines PAC. The dashed dotted curve is calculated by means of Eq. (37), combining the tilted geometry with the PAC calculation. In the other panels: Long dashes: TAC, dotted lines: BFFP, open circles: RMB dashed dotted lines: FM

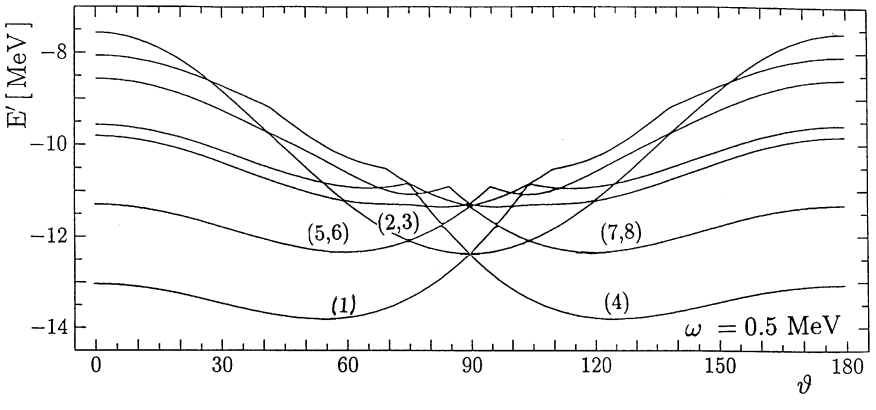

Fig. 13. Routhian as a function of the tilt angle for the combination of a DAL proton hole with a DAL neutron hole

band (3, 4) is just about to start (very shallow minimum at 34°) and (4, 5) has not started yet (minimum lies at 0°). This agrees with the beginnings of the corresponding the PRM curves in Fig. 15. For $\omega = 0.9$ MeV, the minima of the configurations 1 and 2 lie at 83° and 97°. The approach of 90° shows up as the onset of signature splitting in the PRM energies. The configurations 7 and 8 correspond to the particle on level 1 and the hole on level 9 and 10. They come down relative to the configurations 3–6. The reason is evident from Fig. 1. The splitting between the RAL levels 1 and 2 and between 1 and 3 grows linearly with ω, whereas the splitting between the DAL levels 12 and 13 and between 9 and 10 does not change very much with ω. In accordance one can see in the upper panel of Fig. 15 the bands (7) and (8) come down and cross bands (3, 4) and (5, 6). For $\omega = 0.7$ MeV the minima of the configurations (7) and (8) reach 90°. Accordingly, we interpret configuration (7) as the $\alpha = 0$ (even I) and 8 as the $\alpha = 1$

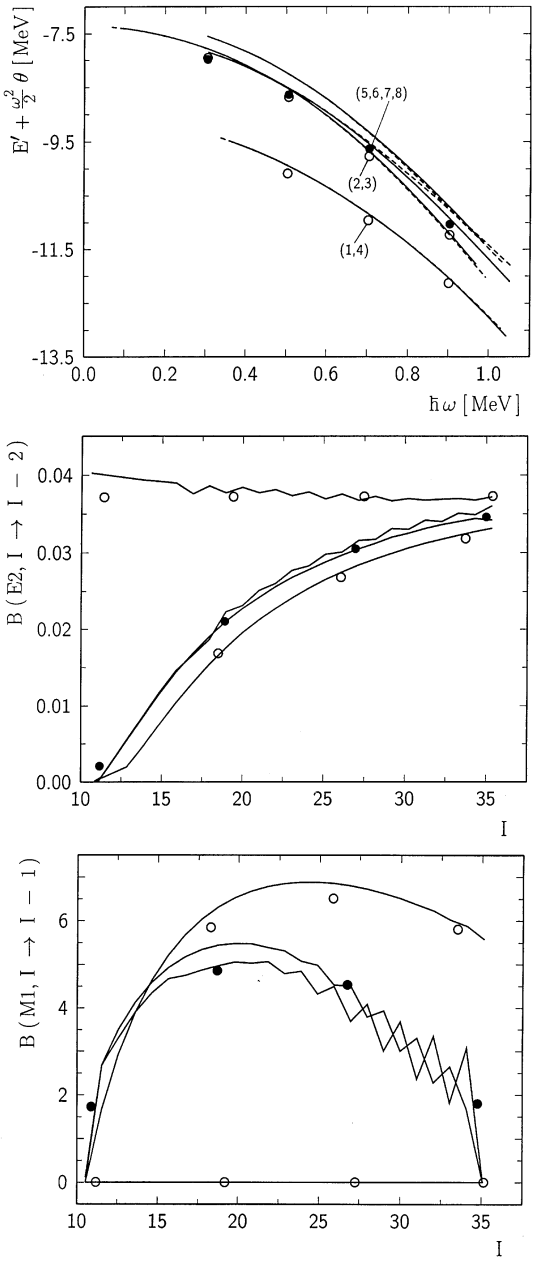

Fig. 14. Excitation spectrum of the combination of a DAL proton hole with a DAL neutron hole. The upper panel shows the Routhians calculated by means of (21) and (22) from the PRM energies. A rigid rotor contribution with $\theta = 30\,\mathrm{MeV}^{-1}$ is subtracted from the Routhian. Full drawn lines correspond to even spin ($\alpha = 0$) and dashed lines to odd spin ($\alpha = 1$). The cranking results are shown by circles, where open circles denote one $\Delta I = 1$ TAC band and closed circles denote two $\Delta I = 1$ TAC bands of the same energy. The TAC configurations are labeled in the same way as in Fig. 13. In the lower two panels only full lines are used for the PRM results (no specification of the signature)

(odd I) band. In the PRM calculation the signature splitting of these two bands sets in at somewhat lower ω. At $\omega = 0.9\,\mathrm{MeV}$ the signature splitting between the bands (7) and (8) agrees well with the one estimated from the cranking calculations. For the other configurations the symmetric minima are still sufficiently far from 90°, such that the TAC interpretation applies. This is in accordance with the small signature splitting the PRM gives for these bands. The example demonstrates that the coexistence and crossing of TAC and PAC bands can be treated in the cranking approach when applying the rules to avoid over counting.

The excitation spectrum of a FAL quasi proton combined with a FAL quasi neutron is shown in Fig. 16 and the right part of Table 1 lists the lowest configurations. For low ω the TAC interpretation applies. The configurations (1, 2) correspond to a $K = 7$, $\Delta I = 1$ band and (3, 4) to a $K = 0$, $\Delta I = 1$ band. The configurations (5, 6, 7, 8) give rise to two $K = 6$ $\Delta I = 1$ bands. They are degenerated in the TAC scheme, but split in the PRM calculation by the recoil term. Around $\omega = 0.7\,\mathrm{MeV}$ one must change to the PAC interpretation. Now all configurations at 90° are accepted and assigned to $\Delta I = 2$ bands, according to the signatures given in the table. As seen, at $\omega = 0.9\,\mathrm{MeV}$ the PAC interpretation works rather well. Again the degenerated PAC configurations (3, 4) are split in the PRM calculation by the recoil term.

The combination of two FAL quasi protons is also shown in Fig. 16. Only the configurations given in the table are allowed by the Pauli principle. Otherwise the cranking results are identical with the case of unlike particles, discussed above. However, the interpretation is different. From the bundle (1, 2, 3, 4) only configuration 3 remains, which has its minimum at 90°. Accordingly, it is interpreted as an even spin PAC band. It represents the well known s-band.[6] At low ω, configurations (5) and (7) have minima symmetric to 90°. Accordingly, they are interpreted as a $\Delta I = 1$ band, which corresponds to the t-band discussed in [3]. Around $\omega = 0.7\,\mathrm{MeV}$ the two minima approach 90° and one must shift to the PAC interpretation, which assigns (5) and (7) to an odd spin and even spin band, respectively. The PAC interpretation becomes more accurate at $\omega = 0.9\,\mathrm{MeV}$. The TAC description is not as good as for the lowest bands in the case of unlike FAL quasi particles. At low ω, the PRM calculation gives already a substantial splitting of the two signature branches of the t-band, which is in contrast to the TAC calculation. The origin of the discrepancy can be traced back to the interaction of the t-band with the s-band, which is seen as the quasi crossing of the configurations (3) and (5) at 68° in the middle panel of Fig. 16. At low ω the energy difference between the s- and the t-band is small and the interaction causes a repulsion. However, this interaction can only act between even spin members, because the s-band has only even spins. Thus, the even spin part of the t-band is pushed up, whereas the odd spin part remains unshifted. This results in a signature splitting. The PRM wave functions show indeed a strong mixing of low- and high-K components for even spins, whereas for odd spins the wave function is centered around $K = 7$.

[6] The PRM calculation does not show its crossing with the g-band, because the 0 quasi particle configuration is not included

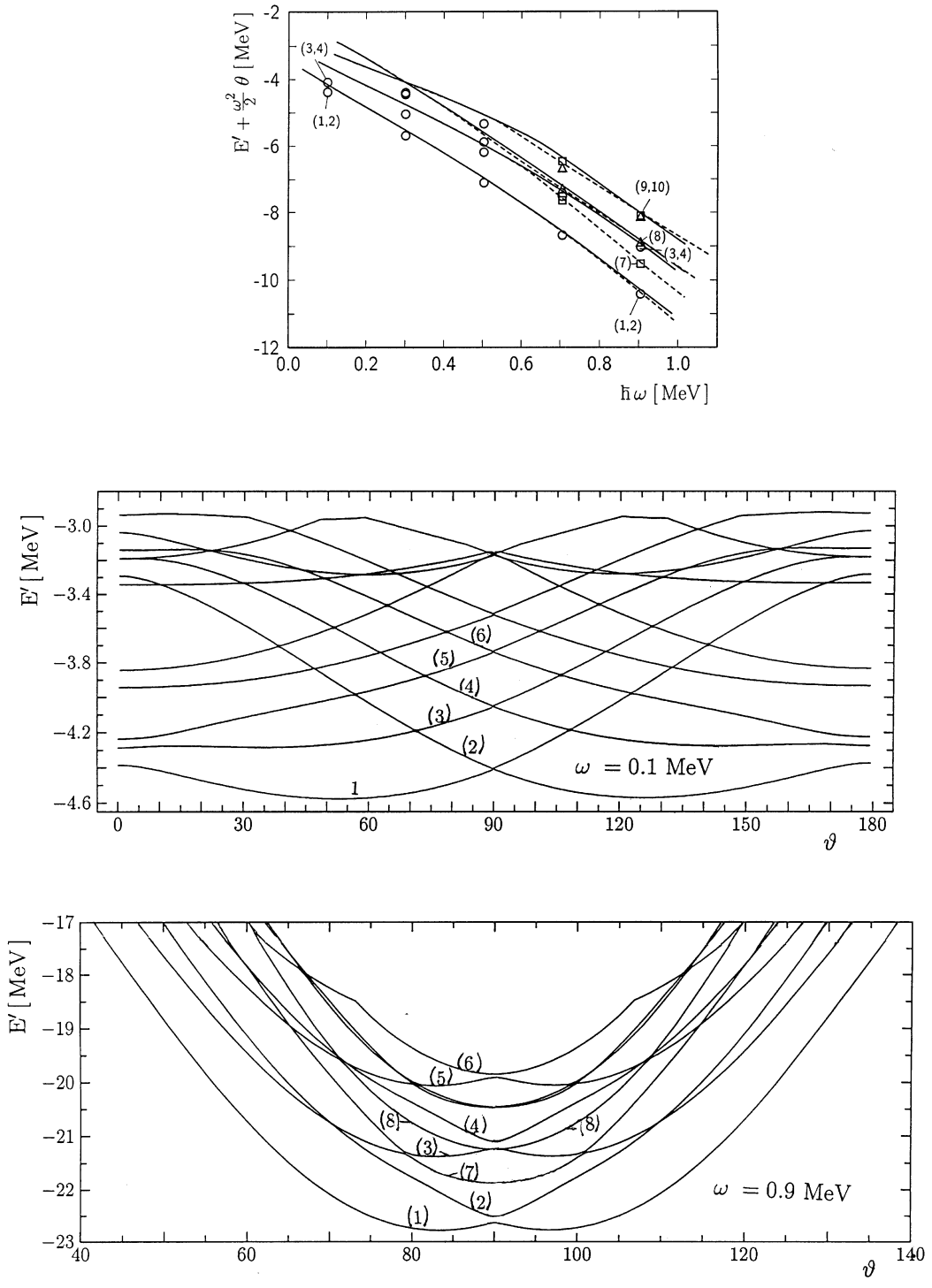

Fig. 15. Upper panel: Excitation spectrum the combination of a RAL proton with a DAL neutron hole. The Routhians are calculated by means of (21) and (22) from the PRM energies. A rigid rotor contribution with $\theta = 30\,\mathrm{MeV}^{-1}$ is subtracted from the Routhian. Full drawn lines correspond to even spin ($\alpha = 0$) and dashed lines to odd spin ($\alpha = 1$). Circles denote a TAC solutions (both signatures), squares and triangles PAC solutions with $\alpha = 0$ and 1, respectively. Lower panels: The cranking Routhians as functions of the tilt angle (no specification of the signature). The configurations are labeled in the same way in all panels

3.7 Construction rules for the excitation spectrum

We have discussed in detail that the cranking configurations must be interpreted differently if the tilt angle is 90° (PAC) or deviates from this value (TAC). The coexistence of TAC and PAC minima in the excitation spectrum and the fact that with increasing frequency the TAC minima approach 90° make it necessary to bring the two

Table 1. The lowest configurations of a RAL proton and a DAL neutron hole (left columns) and two FAL quasi particles (right columns). The single particle or quasi particle states are labeled as in 1. The first and fourth columns enumerate the configurations, the second, fifth and sixth columns indicate the configurations and the third and seventh columns give the signature of the configurations at $\vartheta = 90^\circ$

conf.	π	ν^{-1}	α	conf.	π	ν	π	π	α
1	1	12	1	1	1	1			1
2	1	11	0	2	2	2			1
3	2	12	0	3	1	2	1	2	0
4	2	11	1	4	2	1			0
5	3	12	1	5	1	3	1	3	1
6	3	11	0	6	3	1			1
7	1	10	1	7	2	3	2	3	0
8	1	9	0	8	3	2			0
				9	1	4	1	4	1
				10	4	1			1
				11	2	4	2	4	0
				12	4	2			0

interpretations into one frame. This can be achieved by the following set of rules:

1. Consider the Routhians $E'(\omega, \vartheta)$ as functions the tilt angle ϑ in the intervals $0^\circ \leq \vartheta \leq 180^\circ$. A minimum is associated with a $\Delta I = 2$ band.
2. For $\vartheta = 90^\circ$ the PAC interpretation applies: The signature of the configuration is known and fixes I mod 2.
3. For minima at $\vartheta \neq 90^\circ$ the TAC interpretation applies: For each minimum at $\vartheta < 90^\circ$ there is one with the same energy at $180^\circ - \vartheta$. These two minima combine into two degenerated $\Delta I = 2$ bands of opposite signature, i.e. into a $\Delta I = 1$ band.
4. Minima at 0° and 180° are disregarded. A band starts when the minima begin to move away from 0° and 180° (band head).
5. Configurations with a minimum at $\vartheta \neq 90^\circ$ belong to a group that forms a bundle emerging from $\vartheta = 90^\circ$. Continue the functions $E'(\omega, \vartheta)$ diabatically through 90° (i.e. draw a line with constant slope even if the calculation may connect the configurations in a different way). Each pair of minima symmetric to 90° (including the ones at 90°) of such a bundle generates a $\Delta I = 1$ band (cf. rule 3). Kinks at 90° are disregarded. This is the TAC interpretation of the bundle that eliminates spurious states.
6. When *all* minima of the bundle are close to 90° (say $|90^\circ - \vartheta| < 10^\circ$) change to the PAC interpretation for the *whole* bundle. Now the diabatic construction of rule 5 is abandoned. Each configuration at 90° (also if maximum) is interpreted as a $\Delta I = 2$ band with I mod 2 given by the signature.
7. PAC interpretation is applied to all minima at $\vartheta = 90^\circ$ that do not belong to bundles.
8. Calculate the $B(M1)$ values by means of (23) if the TAC interpretation applies and by means of (25) if PAC interpretation applies.
9. Calculate the $B(E2)$ values by means of (24), irrespective of the interpretation.

4 Treatment of $K \neq 0$ bands in PAC

Conventionally, *all* bands have been described in the frame of the PAC. In the case of the high-K bands, the problem is encountered that the expectation value $J_3 = i_3 = 0$. This follows from the conservation of signature [10]. The finite value of K causes substantial corrections to the energies and, in particular, to the transition rates. In order to be able to describe the bands with finite K within PAC, two recipes have been used to estimate J_3. Ring et al. [9] (referred to as RMB) suggest

$$J_3 = \sqrt{\langle |j_3^2| \rangle}, \tag{30}$$

where the expectation value is calculated as a function of ω. Bengtsson and Frauendorf [10] and Fässler and Plozajczak [11] (referred to as BFFP) assume

$$J_3 = K, \tag{31}$$

where K is kept constant, equal to the band head spin. The latter approach may be viewed as an approximation to the TAC, which assumes that i_3 does not change as a function of ω. This assumption is justified if the particles responsible for i_3 are sufficiently strongly coupled to the deformed field. Both recipes are used to obtain the energies $E(J)$ from $E(J_1)$, calculated by means of PAC, where (19) is used to express J in terms of J_1. Applying the approximation BFFP to the TAC expressions (23, 24) for the $B(M1)$ and $B(E2)$ values, one obtains the vector model of Dönau and Frauendorf [12] (referred to as DF) for the transition probabilities. This becomes evident from[7]

$$\cos \vartheta = \frac{J_3}{J} = \frac{K}{I + 1/2}. \tag{32}$$

Comparing PAC with the PRM, we found a third recipe to give the best approximation (referred to as FM). The i_3 values are calculated for each particle separately by means of the expression

$$i_{3\,p(n)} = \sqrt{\langle p(n) | j_3^2 | p(n) \rangle}. \tag{33}$$

Their sum is J_3. The individual values of i_3 are used in (23) to calculate the $B(M1)$ values.

[7] In [12] the angle $\alpha = 90^\circ - \vartheta$ is used

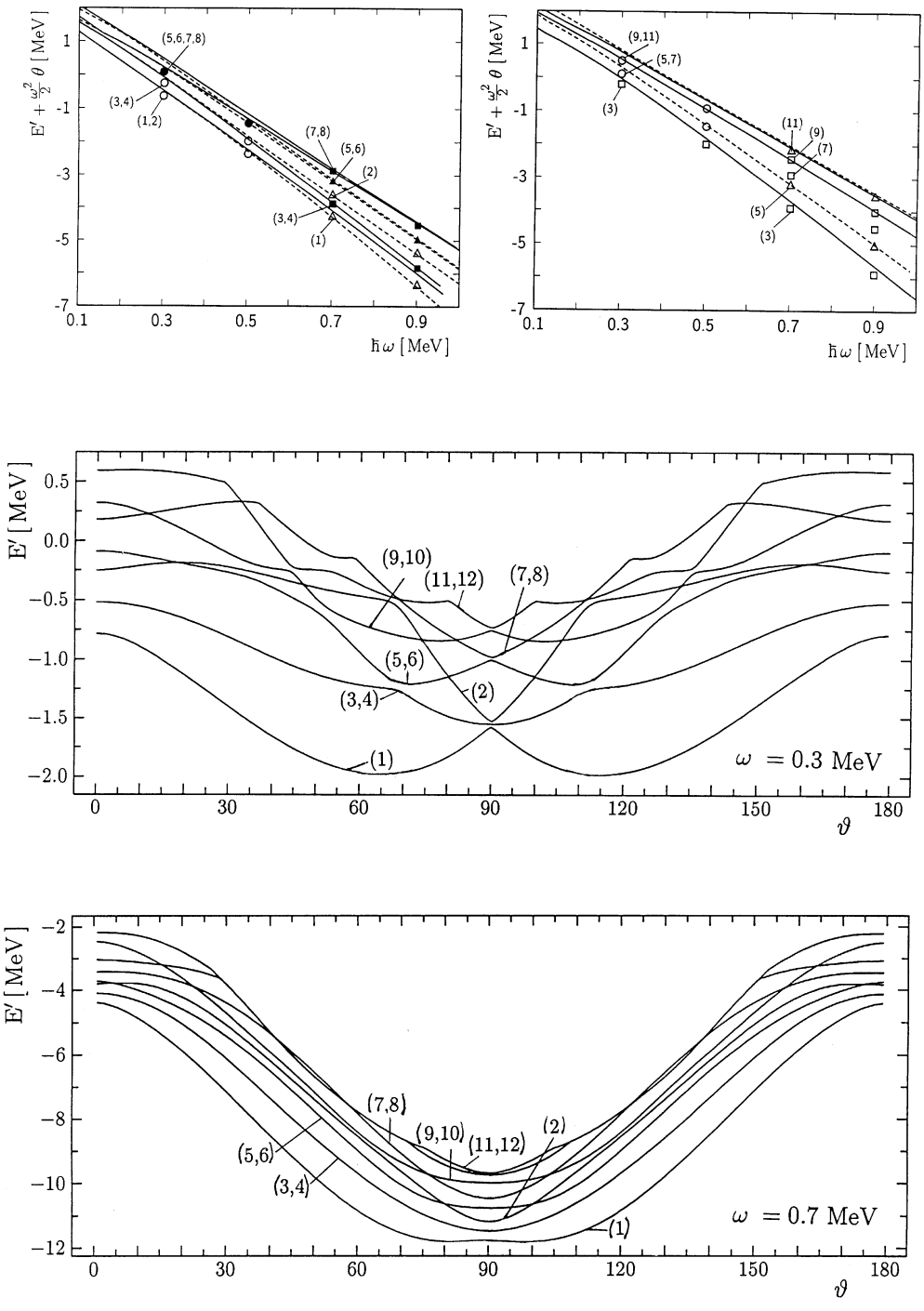

Fig. 16. Upper left panel: Excitation spectrum of the combination of a FAL proton with a FAL neutron hole. Upper right: Excitation spectrum of the combination of a two FAL protons or neutrons (upper right). The Routhians are calculated by means of (21) and (22) from the PRM energies. A rigid rotor contribution with $\theta = 30$ MeV^{-1} has been subtracted from the Routhian. Full drawn lines correspond to even spin ($\alpha = 0$) and dashed lines to odd spin ($\alpha = 1$). Circles denote a TAC solutions (both signatures), squares and triangles PAC solutions with $\alpha = 0$ and 1, respectively. Full symbols denote two fold degeneracy. Lower panels: The cranking Routhians as functions of the tilt angle (no specification of the signature). The configurations are labeled in the same way in all panels

As seen in Figs. 6 and 12, BFFP works well at lower ω, where $\boldsymbol{i}$ does not deviate very much from the 3-axis. The drop of the $B(M1)$ values at high spin cannot be obtained assuming a fixed J_3, because it is a consequence of the reorientation of $\boldsymbol{i}$ towards $\boldsymbol{J}$. This reorientation increases the tilt angle ϑ and the $B(E2)$ value. Hence, the fixed K prescription, gives very good results in the lower part of a band but becomes progressively inaccurate with increasing spin.

RMB that uses $J_3 = \sqrt{\langle j_3^2 \rangle}$ works well for the case of one quasi particle (cf. [9 13]).[8] However, as seen in Figs. 6 and 12, it deviates considerably from the PRM in the case of two quasi particles. Near the band head a one quasi particle state of good signature is given by

$$|\pm\rangle \approx \frac{1}{\sqrt{2}}(|k\rangle \pm |-k\rangle), \quad \langle \pm |j_3^2| \pm \rangle \approx k^2, \tag{34}$$

what amounts to $J_3 \approx k$. For the lowest two quasi particle states

$$|\pm\pm\rangle \approx \tfrac{1}{2}(|k_p\rangle \pm |-k_p\rangle)(|k_n\rangle \pm |-k_n\rangle) \tag{35}$$

and one finds

$$J_3 = \sqrt{\langle \pm\pm |j_3^2| \pm\pm \rangle} \approx \sqrt{\tfrac{1}{2}(k_p^2 + k_n^2)} \tag{36}$$

instead of $J_3 \approx k_p + k_n$. Thus, for multi quasi particle states RMB fails. As can be seen in Figs. 6 and 12, the version FM suggested in this paper avoids this problem, because J_3 is calculated as the sum of the individual contributions $i_{3p(n)} = \sqrt{\langle p(n)|j_3^2|p(n)\rangle}$.

One may modify the PAC expression (25) for the $B(M1)$ values in order to incorporate the tilted geometry,

$$B(M1) = \frac{3}{8\pi}[(g_\tau - g_R)(\sqrt{2}\langle 1|j_{\pm 1\tau}|2\rangle + (\sin\vartheta - 1)i_{3\tau}) - \cos\vartheta((g_p - g_R)i_{1p} + (g_n - g_R)i_{1n})]^2, \tag{37}$$

$$i_{3\tau} = \langle 1|j_{3\tau}|2\rangle, \cos\vartheta = i_{3\tau}/J_1. \tag{38}$$

For the case of one quasi particle, this expression essentially agrees with the modification of the DF formula, suggested by Dönau [13] in order to describe signature effects.[9] As demonstrated there and in Fig. 4, it describes rather well the $B(M1)$ values in the whole spin range, including the signature staggering. However, this is not the case for two quasi particles, as shown in Fig. 12. Though it somewhat improves the $B(M1)$ values in the PAC limit it fails at low spin and it does not merge the TAC results any better than the uncorrected expression (25). Hence, it seems only to be possible to construct an $B(M1)$ expression that describes both the tilted geometry and the signature staggering if the J_3 component of the angular momentum is generated by *one quasi particle*. This should be taken as a warning when analyzing data in terms of the DF formula, using alignments estimated from the experimental spectra. Only for the cases when J_3 comes from just one quasi particle, one may incorporate the signature splitting by means of (37). If this is not the case one must use the original DF expression (23). which does not describe the signature dependence of the $B(M1)$ values, but only averages over the two signatures.

[8] Comparing the PRM with PAC, [13] had to introduce a shift in angular momentum in order to match the results. This turns out to be unnecessary in our comparison. The reason is that we keep the recoil term in our PRM in contrast to [13]

[9] The term sin $\vartheta i_{3\tau}$ in Dönau's expression corresponds to a somewhat different ϑ value

5 Conclusions

Comparing with the results of a Particle Rotor Model calculation, we find that the Tilted Axis Cranking approach quantitatively accounts both for the energies and the intra band transition rates of the lowest bands generated by one or two quasi particles coupled to an axial rotor. It is expected that Tilted Axis Cranking works with comparable accuracy for multi quasi particle bands, which are difficult to describe in the frame of the Particle Rotor Model.

Tilted Axis Cranking provides an accurate description of the band head, except in cases, when substantial alignment of quasi particle angular momentum occurs at very low frequency.

The interpretation of the Cranking results suggested in [3], which associates minima at a tilt angle $\vartheta \neq 90^\circ$ with $\Delta I = 1$ bands and such at 90° with $\Delta I = 2$ bands of the appropriate signature, turned out to be correct. The interpretation has been refined by a set of rules that permits to construct the excited bands from the cranking configurations. Applying these rules leads to a one to one correspondence with the low lying bands of the Particle Rotor Model calculations. No spurious configurations are generated.

The main draw back of the Tilted Axis Cranking theory is the necessity to switch between two different interpretations. Such change of interpretation is always necessary when the mean field solution breaks spontaneously a symmetry. In the considered case the C_2 symmetry is broken and the signature quantum number lost. As a consequence, the Tilted Axis Cranking theory cannot describe the gradual onset of signature splitting, which appears discontinuously when changing from the TAC to the PAC interpretation. Sufficiently far from the discontinuity the energies and transition probabilities are quite well reproduced by the semi classical expressions. The transition region may be bridged by interpolation in a qualitative way. Other quantities like mixing ratios, static magnetic moments and quadrupole moments, have also been studied. Tilted Axis Cranking describes them with comparable accuracy as the $B(M1)$ and $B(E2)$ values, discussed.

As in the standard cranking theory, the mixing of bands with substantially different quasi particle angular momentum cannot be described by Tilted Axis Cranking.

Previous schemes to account for finite angular momentum along the symmetry axis that stay within the frame of rotation about the principal axes have been investigated. Generally they agree less well with the Particle Rotor Model than the Tilted Axis Cranking approach. An exception is the case of one quasi particle, where they work well and provide even a description of the signature effects. However, for two quasi particles this is generally no longer the case.

The particle rotor model was used in this study as an "exact model" against which the semi classical Tilted Axis Cranking was checked. The aim was to outline the limitations of Tilted Axis Cranking due to the violation of angular momentum conservation and to test its accuracy. Tilted Axis Cranking is a microscopic theory that in many respects goes far beyond the Particle Rotor Model. For

example, one may easily study multi-quasi particle excitations, and the consequences of changes of the deformation or the pairing. Furthermore, it gives transparent classical pictures of the angular momentum coupling.

The authors would like to thank F. Dönau for numerous discussions during the completion of this work. J.M. would like to thank FZR for the fellowship and the hospitality extended to him. He is also partly supported by the National Science Foundation in China.

References

1. Frisk, H., Bengtsson, R.: Phys. Lett. B**196**, 14 (1987)
2. Frauendorf, S., Bengtsson, T.: Int. Symp. on Future Directions in Nuclear Physics, Strasbourg 1991, AIP Con. Proc. 259, p. 223
3. Frauendorf, S.: Nucl. Phys. A**557**, 259c (1993)
4. Frauendorf, S., Meng, J., Reif, J.: Proc. Conf. on Phys. from Large γ Ray Detectors, Berkeley 1994, p. 54
5. Brokstedt, A. et al.: Nucl. Phys. A**578**, 337 (1994)
6. Baldsiefen, G. et al.: Nucl. Phys. A **574**, 521 (1994)
7. Szymanski, Z.: Fast Nuclear Rotation, p. 29 ff. Oxford: Clarendon Press 1983
8. Bohr, A., Mottelson, B.: Nuclear Structure II, p. 1 ff. New York: Benjamin 1975
9. Ring, P., Mang, H.J., Banerjee, B.: Nucl. Phys. A**225**, 141 (1974)
10. Bengtsson, R., Frauendorf, S.: Nucl. Phys. A**327**, 139 (1979)
11. Fässler, A., Plozajczak, M.: Phys. Rev. C **16**, 2032 (1977)
12. Dönau, F., Frauendorf, S.: Proc. Conf. on High Angular Momentum Properties of Nuclei, Oak Ridge 1982, Nucl. Sci. Res. Con. Ser. V. **4** Harwood NY, p. 143
13. Dönau, F.: Nucl. Phys. A**471**, 469 (1987)
14. Hamamoto, I., Sagawa, H.: Nucl. Phys. A**327**, 99 (1979)
15. Frauendorf, S.: Phys. Scr. **24**, 349 (1981)